23rd ABCM International Congress of Mechanical Engineering
December 6-11, 2015, Rio de Janeiro, RJ, Brazil

EFFECT OF OVERLAP ORIENTATION IN FATIGUE PERFORMANCE OF FRICTION STIR WELDING OF MAGNESIUM SHEETS

J.F.C. Moraes
Department of Mechanical Engineering, The University of Alabama, Box 270276, Tuscaloosa AL 35487-0276
jfmoraes@crimson.ua.edu
R.I. Rodriguez
Department of Mechanical Engineering, The University of Alabama, Box 270276, Tuscaloosa AL 35487-0276
rirodriguez@crimson.ua.edu
J.B. Jordon
Department of Mechanical Engineering, The University of Alabama, Box 270276, Tuscaloosa AL 35487-0276
bjordon@eng.ua.edu

Abstract. *In this work, the effects of sheet stacking orientation on fatigue performance of friction stir welding (FSW) of overlap joints is presented. During FSW, it is well known that the advancing and retreating flow of the material generated by the tool creates asymmetrical weld features. As such, FSW was carried out on 2mm thick AZ31 magnesium alloy sheets, where the orientation of the pull direction of the overlap joint was varied with respect to the tool rotation direction. Load control fatigue tests at R= 0.1 were carried out until full separation of the joint was achieved. Fatigue results showed that the overlap joints loaded on the retreating side exhibited superior performance compared to the advancing side. Microstructure and fractography analysis suggest that the geometrical shape of the faying surface produced by the advancing and retreating flow determines the number of cycles to failure in FSW overlap joints.*
Keywords: *friction stir welding, fatigue, magnesium alloy*

1. INTRODUCTION

The automotive industry worldwide is working on decreasing fossil fuel consumption to address both government regulations and customer demands. One way to achieve these goals is to use materials with enhanced strength-to-weight ratio (Barnes and Pashby, 2000). For example, materials such as aluminum and magnesium, which are known to have high strength-to-weight ratios, have been used in the body-in-white production. In fact, the employment of lightweight materials, like magnesium, can drastically reduce vehicle weight while maintaining satisfactory structural performance. However, traditional joining techniques, such as resistance spot welding (RSW) which is widely applied to join steels, have been demonstrated to be impractical for the joining magnesium alloys (Yan, et al., 2005). This unviability is mainly due to the high electrical and thermal conductivity (Czerwinshi, 2011) characteristic of metals like Mg and Al alloys that require high electrical currents, which in turn lead to poor quality welds. While many alternative joining techniques for magnesium alloys are available, friction stir welding (FSW) is very appealing. FSW is a solid-state process which takes place at temperatures below the melting point of the material, therefore problems related to solidification, such as formation of second phases, porosity, embrittlement and cracking, are not present (Gibson et al., 2014). Moreover, the relatively low temperature at which the process is realized enables it to obtain joints having low distortion and low residual stresses compared to fusion welding (Gibson et al., 2014). In addition, FSW is an energy efficient joining technique and does not require the use of a filler material and typically, no shielding gas.

Among the variations of FSW there is the fillet joint, friction stir spot welding (FSSW) and friction stir linear welding (FSLW). Regarding the FSLW, there can be a butt, T-butt or lap configuration weld. Although the friction stir lap-welding configuration has a high potential use in automotive and aerospace application, limited research has focused on its application and performance (Yuan et al., 2012).

In FSLW, two sheets can be assembled in an overlap configuration, as shown in Figure 1. In this welding configuration, a rotating tool is plunged into the two materials at a determined depth, having the tool shoulder in contact with the top sheet as the tool travels straight along the welding segment. Then, the lap linear weld is finished when the tool is retracted (Yang, Chen, Shi, 2011). Due to the material flow and the travel of the tool, two distinctive features are produced in this type of weld; these are the advancing side and the retreading side of the weld. The advancing side (AS) is the side of the tool where the point velocities are faster (rotation plus translation), whereas the retreating side (RS) is the side of the tool where the pin velocities are slower (rotation minus translation). As shown in Fig.1a and Fig.1b, for the same traveling direction and rotation of the tool, the side of the weld to be loaded is defined according to the orientation of the sheets relative to the pull direction.

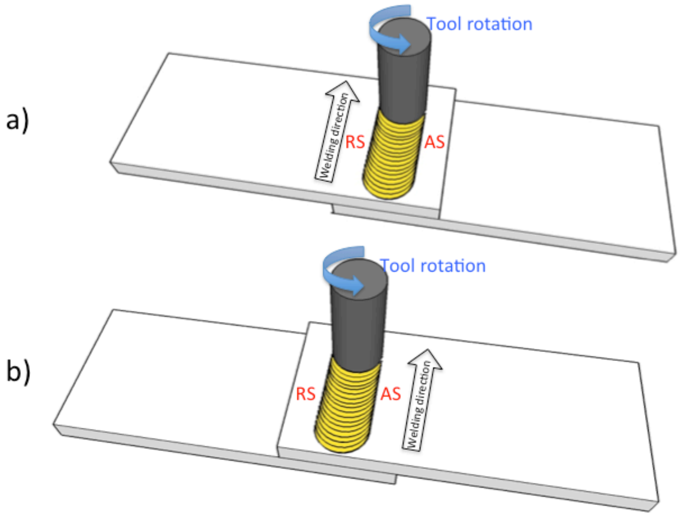

Figure 1. Coupon layout of friction stir lap welding; a) retreating side, b) advancing side.

The faying surface of the AS usually remains exterior to the weld nugget and points upwards along the weld nugget boundary (Yadava et al., 2010). On the other hand, the RS curves upward and enters into the nugget. As the AS takes a hook form, it is called the hooking defect; nevertheless, the RS is known as a cold lap defect (Yadava et al., 2010). It is known that macro features such as the hooking and cold lap formation depend on a combination of tool geometry and welding parameters. Furthermore, it is well known that hooking and cold lap features highly affect the static weld strength and decrease the joint load capacity and/or crack nucleation and propagation (Yuan et al., 2012). As their formation depends on the heat generated from friction between the tool and the pieces to be joined, and material flow during the FSW process, characteristics of FSLW highly depend on tool geometry (Mishra and Ma, 2005). Yadava et al. (2010) studied the effects of tool rotation rate, transverse speed, plunge depth, tilt angle, and pin height on friction stir lap welding on thin aluminum sheets. Commin et al. (2009) investigated the correlation between processing parameters, heat and plastic deformation with microstructure and mechanical properties in AZ31 friction stir butt welds. Yang et al.(2011) studied different tool geometries and process conditions and their influence on shear strength of AZ31 friction stir lap welds. Among their discoveries, it was also found that a higher tensile load is reached when the loading of the RS is on the top sheet. Yuan et al. (2012) evaluated the effect of different tool designs and weld variables, such as welding pitch and plunge depth, on the top sheet thinning (distance from the hook or cold feature to the top surface of the upper sheet) in friction stir lap joints of AZ31. In their study, shear strength for different welding parameters was analyzed. Also, shear strength loading of the AS or the RS of the top sheet was evaluated, which showed that the RS can resist higher loads compared to the AS with the same process parameters. However, durability in fatigue was not analyzed.

While there has been some work focused on the effect of welding parameters and loading conditions on the FSLW in magnesium alloy, the effect of sheet stacking orientation on fatigue performance has not been elucidated. As such, the objective of this paper is to compare mechanical properties as well as fracture characteristics of both AS and RS for magnesium AZ31 alloy joined by FSLW.

2. MATERIALS AND EXPERIMENTS

Commercial grade AZ31 Mg alloy sheets, with a nominal chemical composition of Mg-3.0%wt Al-1.0%wt Zn, having a thickness of 2.0 mm, width of 75 mm and length of 1500 mm were chosen for the present study. The plates were assembled in an overlap configuration and welded at a tool rotational speed of 2000 rpm and a travel speed of 4.6 mm s^{-1}. A welding tool having a concave scroll shoulder with 13 mm diameter and 3.5 mm long tri-flat threaded pin with 4.7 mm pin tip diameter and 6.0 mm pin root was used. Two sets of FSLW were done in an overlap configuration. The only difference between the two sets is the overlap orientation (i.e. the orientation of the top and bottom sheets in order to have the advancing or retreating side on the free edge of the top sheet). A schematic drawing of the coupons are shown in Fig. 2. As can be seen, the plates were cut into 30 mm wide and 120 mm long coupons for mechanical testing purposes.

A MTS 809 servo hydraulic was used to perform lap shear tensile tests (quasi-static) for each weld configuration in order to obtain a representative average maximum load carried for each condition. Four specimens were tested per configuration. A grip-to-grip distance of 60 mm, at an actuator speed of 1mm min^{-1} was used during tensile testing. For fatigue testing, the specimens were tested with the same grip-to-grip distance in an MTS-312 with a 2224 N (500 lbf) load cell, under load control condition with a sinusoidal waveform at load ratio R=0.1 and frequency 20 Hz. Mg sheet shims were used in order to avoid additional bending moments and loads.

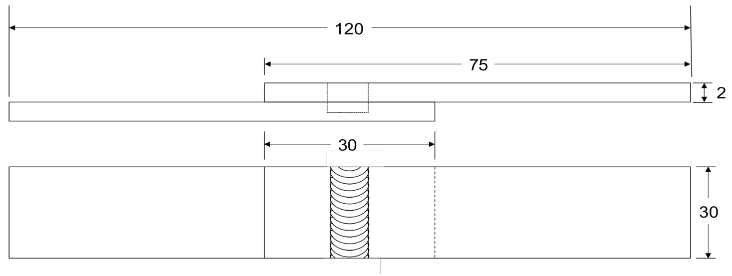

Figure 2. Configuration of the friction stir linear welded lap-shear coupon. Dimensions are in millimeters.

Regarding asymmetric geometrical features, Reynolds and Cederqvist (2001) proposed two different arrangements in order to load a friction stir linear weld: a) RS loading and b) AS loading. These two dissimilar configurations are depicted in Fig. 3. The shims used to avoid adding additional moments loads and the axial forces are also shown in this scheme.

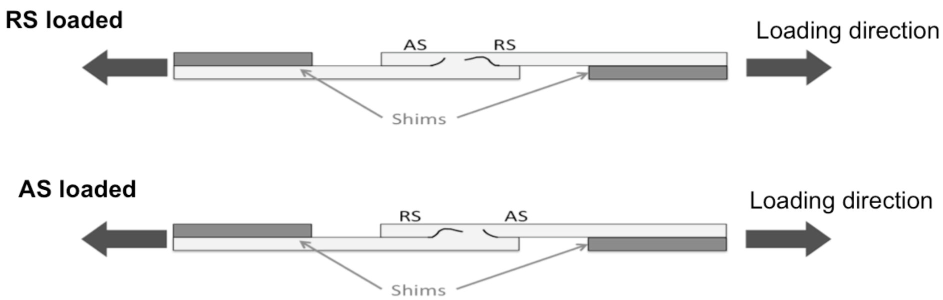

Figure 4. Schematic loading configurations: a) RS and b) AS.

In addition to mechanical testing, weld and failure characterization were performed. Tested and untested samples were sectioned parallel to the loading direction, cold mounted in epoxy, grounded and polished. The final polishing was done on a neoprene pad with alumina 0.05 micron in glycol slurry. In order to analyze the microstructure, the mounted specimens were etched using a solution composed of 4.2 g picric acid, 10 ml acetic acid, 10 ml H_2O and 70 ml ethanol (Jordon et al. 2010; Afrin et al.2008). An optical digital microscope Keyence VHX-1000 was used to evaluate size and shape of the hooks of the weld, effective sheet thickness and transverse crack propagation under different loading conditions. Microhardness measurements were done throughout the mounted specimens on both the top and bottom sheets with increments of approximately 0.5 mm also, using a Wilson hardness testing machine. A load of 100 g with a dwell time of 5 seconds was applied in order to obtain the Vickers hardness (HV) along the specimen. For crack nucleation and propagation analysis, failed surfaces of coupons were examined in a Jeol 7000 scanning electron microscope (SEM).

3. RESULTS AND DISCUSSION

The cross-section of an as-welded specimen is presented in Fig. 4. Due to the relative velocity of the tool to the coupon during the welding process, the resulting cross section of the coupon is not symmetric. The faying surface on the advancing side (AS) usually has the shape of a hook and it curves upwards along the nugget periphery, On the other hand, the faying surface on the retreating side (RS) extends through the welding nugget towards the AS, as this feature is generally referred to as the cold lap feature (Yuan et al. 2012). On the extension side of the hook and along the cold feature, there are oxide layers that originated from the surface of the contact between the sheets prior to the welding processes. The oxide layers, hook on the AS, and the cold lap feature originated on the RS are shown in Fig. 4.

It is important to note that the hooking features depend on relative velocities between the tool and coupon. The horizontal and vertical flow of material determines whether the hook curves upward or downward. The material in front of the rotating tool is pushed upward due to its tilt angle. The amount of material being driven upward on the leading side flows around the pin in the rotation direction (Schmidt, Dickerson, and Hattel, 2006; Colligan, 1999; Seidel and Reynolds, 2001), resulting in a hook that points toward the tool pin (Fig. 4a). Furthermore, this material flow decelerates on the trailing side while being accumulated in the void of the stir of the pin (Colligan, 1999), and developing a hook pointing downwards (away from the tool pin), as demonstrated by the faying surface of the RS is shown in Fig.3c. Cold lap features are observed through the weld nugget (Fig.4b).

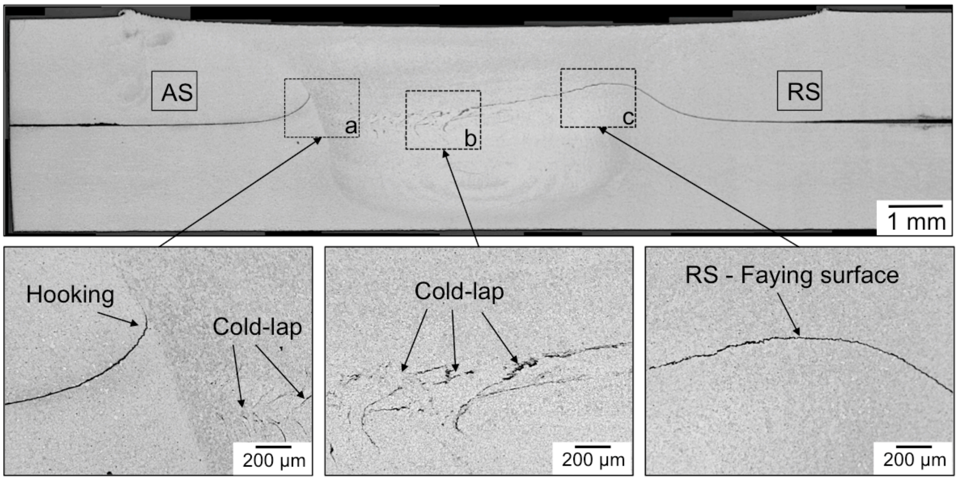

Figure 4. Cross-section of a friction stir linear weld in lap configuration where AS is the advancing side and RS is the retreating side.

Prior to fatigue testing, tensile test were performed in order to reveal the maximum average peak load supported by each type of loading configuration. Similarly, Yuan et al. (2012) analyzed maximum loads reached for AS and RS loading with different welding parameters, and found that the maximum load for the RS loading condition was higher than the AS with the same parameters in all three cases studied. Even though the welding parameters in the presented study are different from Yuan et al. (2012) study, the average maximum peak load of the RS was 54% greater than the one of the AS. The force-displacement curves under quasi-static shear testing are shown in Fig. 5.

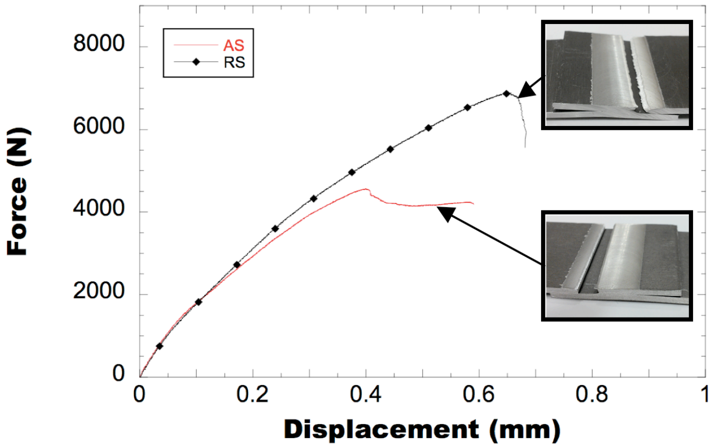

Figure 5. Force versus displacement curves for quasi-static tensile test loading of the retreading side (RS) and advancing side (AS).

Figure 6 shows the plot of the maximum load applied versus the number of cycles to failure (i.e. complete separation of the tested coupon). The arrows on a data point indicate that the test was stopped at that number of cycles and the specimen had not failed. It can be observed that the RS loading configuration exhibited significantly longer fatigue lifetimes compared to the AS loading configuration. If the data points of non-failed coupons from Fig. 6 are excluded, and remaining data is divided by the average maximum load obtained from quasi-static tests for the same loading configuration (i.e. AS or RS loading configuration), a normalized plot can be created. Figure 7 shows a normalized plot of the maximum load applied on fatigue test divided by the maximum average load obtained from tensile test versus the number of cycles to failure. It can be clearly seen that the differences observed Fig. 6 collapse into a single curve. This is a significant point since, it suggests that for FSLW of similar alloy, the fatigue difference associated with specific welding parameters appears to be correlated directly with static strength of the joint. However, more experiments are needed to test this hypothesis.

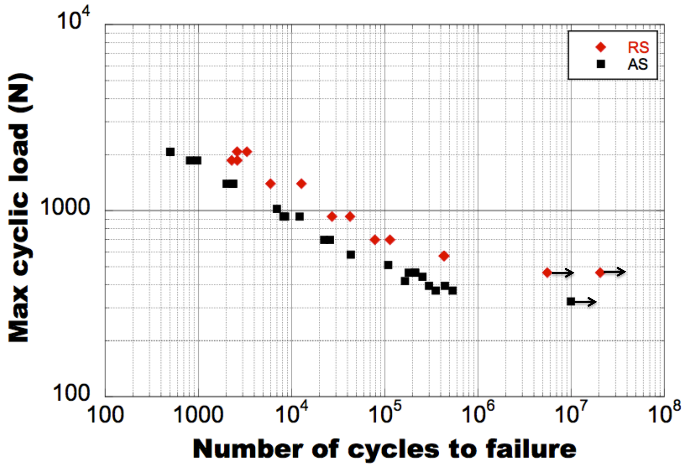

Figure 6. Experimental results of the maximum cyclic load versus the number of cycle to failure of the specimen at load ratio R=0.1.

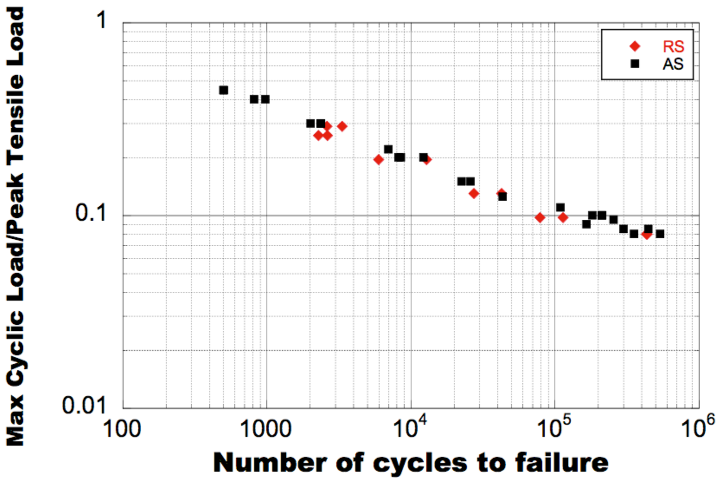

Figure 7. Experimental results of the maximum cyclic load divided by the average peak value, obtained from quasi-static tensile test, versus the number of cycle to failure of the specimen at load ratio R=0.1.

Regarding fracture mode of the coupons under mechanical loading, Fig. 8 shows the cross-section of failed coupons at different load conditions. In Figs. 10a-c, the advancing side of the weld was loaded while Figs. 10d-f, shows the case where the retreading side of the weld was loaded. Even though the AS and RS configurations are dissimilar and the load magnitudes for the RS are substantially higher than the ones for the AS in order to obtain the same fatigue life, the crack propagation and failure mode of both the AS and RS exhibited similar fracture characteristics. Figures 10a and 10d show the failed cross-section of coupons under quasi-static testing, where a typical ductile failure was observed in the SZ, and a high amount of twinning was observed. According to Yang et al. (2011), this type of failure is due to localization of deformation, indicated by mechanical twins near the fractured surface.

Low cycle fatigue failure of the AS is show in Fig. 10b with failure at 503 cycles and maximum load of 2,069 N. The low cycle fatigue failure of the RS occurred at 2,620 cycles at a maximum load of 2069 N as shown in Fig. 10e. In both cases, cracks grew directly through the stir zone and into the surface of the top sheet. Also, lower amount of twinning occurred compared to tensile loading. The high cycle fatigue failures are shown in Fig. 10c, where failure of the AS occurred at 353,589 cycles at maximum load of 371 N. Fig. 10f shows the failure of the RS at 437,661 cycles at a maximum load of 570 N. It is important to note that at under lower applied amplitudes, the crack propagates trough the boundary between the stir zone and thermo-mechanically affected zone in both conditions, and evidence of twinning is basically non-existent.

Figure 9 shows SEM images of fracture surfaces of AS and RS loaded in similar conditions: Fig. 9a shows the AS, where failure occurred at 43,368 cycles at a maximum load of 580 N. In Fig. 9b, the RS failed at 432,166 cycles at maximum load of 570 N. Failed specimens under different load conditions were also analyzed, however the crack initiation and propagations were observed to be similar to what is shown in Fig. 9. For the AS, the crack initiates at multiple locations across the hook tip, and then it grows towards the top surface. For the RS, crack nucleation and propagations are very analogous, however multiple crack initiation locations occur through the closest faying surface of the RS hook to the free surface top sheet, instead of the hook tip.

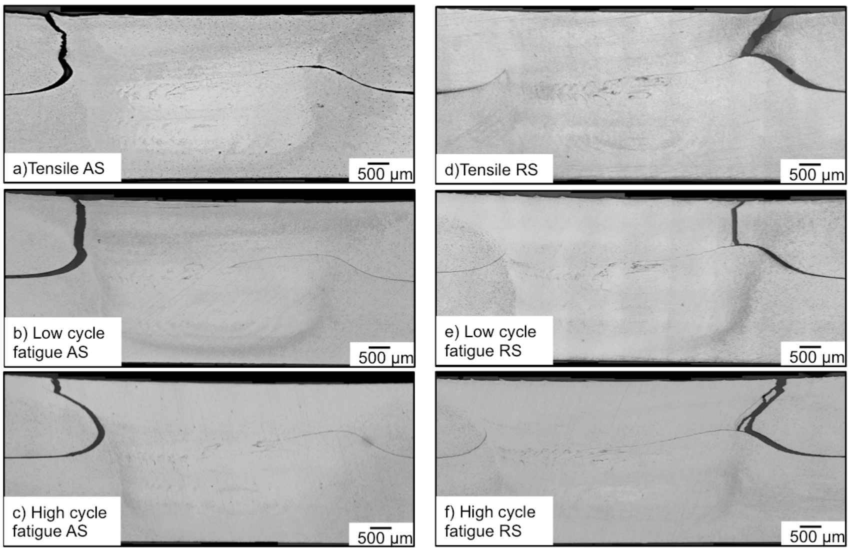

Figure 8. Failed specimens loaded on the advancing side: a) tensile, b) fatigue at 503 cycles and maximum load of 2,069 N, c) fatigue at 353,589 cycles and maximum load of 371 N. Failed specimens loaded on the retreating side: d) tensile, e) fatigue at 2,620 cycles and maximum load of 2,069 N, f) fatigue at 437,661 cycles and maximum load of 570 N. All fatigue testing was performed at R=0.1.

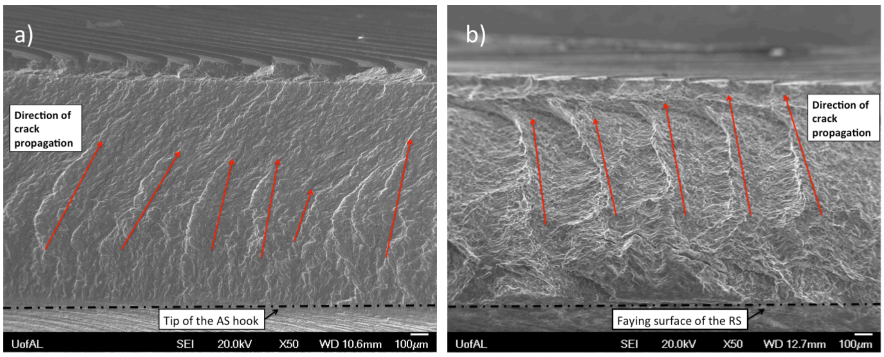

Figure 9. Scanning Electron Microscopy of fracture surfaces of AZ31 mg alloy joined by FSLW. a) AS, failed at 43,368 cycles at a maximum load of 580 N, b) RS, failed at 432,166 cycles at a maximum load of 570 N with R= 0.1. Multiple crack initiation points and crack propagation direction is shown.

4. CONCLUSIONS

Mechanical testing was performed on friction stir linear welding (FSLW) of AZ31 mg alloy sheets. In this study, two sets of coupons were generated to characterize FSLW properties upon loading the advancing or retreading side of the joint. Experimental results revealed that greater fatigue life, up to an order of magnitude, was achieved when loading the retreading side compared to the advancing side load configuration. However, the the fracture modes of both coupons exhibited very similar modes of failure The fracture mode in both configurations initiated at multiple locations- on the hook tip for the AS and on the closest faying surface to the surface of the top sheet for the RS, which grew in direction to the top surface of the top sheet. A normalized curve of maximum cyclic load divided by the average maximum tensile load versus the number of cycles to failure was generated reveling that both loading conditions lay in the same line, thus making it possible to estimate the fatigue life of this particular weld and the corresponding over-lap configuration. Based on the results from the present study, it suggests that the behavior of a FSLW loaded on the AS or RS depends mostly on the macro features (i.e. hooking and faying surface) rather then on microstructure.

5. ACKNOWLEDGEMENTS

The authors would like to thank Blair Carlson, and Robert Szymanski for the fabrication of the FSLW samples. In addition, the authors want to recognize members of the United States Automotive Materials partnership (USAMP) Magnesium Front End R&D project, including Joy Forsmark, Jim Quinn, Robert McCune, Xuming Su, AK Khosrovaneh, and Yung-Li Lee for their helpful discussions. This material is based upon work supported by the Department of Energy, National Energy Technology Laboratory under Award Number No. DE-EE0005660. This report was prepared as an account of work sponsored by an agency of the United States Government. Neither the United States Government nor any agency thereof, nor any of their employees, makes any warranty, express or implied, or assumes any legal liability or responsibility for the accuracy, completeness, or usefulness of any information, apparatus, product, or process disclosed, or represents that its use would not infringe privately owned rights. Reference herein to any specific commercial product, process, or service by trade name, trademark, manufacturer, or otherwise does not necessarily constitute or imply its endorsement, recommendation, or favoring by the United States Government or any agency thereof. The views and opinions of authors expressed herein do not necessarily state or reflect those of the United States Government or any agency thereof. Such support does not constitute an endorsement by the Department of Energy of the work or the views expressed herein. This work utilized resources owned and maintained by the Central Analytical Facility, which is supported by The University of Alabama.

6. REFERENCES

Afrin, N., Chen, D. L., Cao, X., & Jahazi, M. (2008). Microstructure and tensile properties of friction stir welded AZ31B magnesium alloy. *Materials Science and Engineering: A*, *472*(1–2), 179–186. http://doi.org/http://dx.doi.org/10.1016/j.msea.2007.03.018

Barnes, T. A., and Pashby, I. R. (2000). Joining Techniques for Aluminum Spaceframes Used in Automobiles Part II—Adhesive Bonding and Mechanical Fasteners. *J. Mater. Process. Technol.*, *99*, 72–79.

Cederqvist, L., & Reynolds, A. (2001). Factors Affecting the Properties of Friction Stir Welded Aluminum Lap Joints. *Welding Journal Research Supplement*, *80*, 281– 287.

Colligan, K. (1999). Material flow behavior during friction welding of aluminum. *Weld J*, (July), 229–237. Retrieved from http://files.aws.org/wj/supplement/WJ_1999_07_s229.pdf

Commin, L., Dumont, M., Masse, J.-E., & Barrallier, L. (2009). Friction stir welding of AZ31 magnesium alloy rolled sheets: Influence of processing parameters. *Acta Materialia*, *57*(2), 326–334. http://doi.org/10.1016/j.actamat.2008.09.011

Czerwinski, F. (2011). Welding and Joining of Magnesium Alloys. In F. Czerwinski (Ed.), *Magnesium Alloys - Design, Processing and Properties* (pp. 469–491). Intech.

Gibson, B. T., Lammlein, D. H., Prater, T. J., Longhurst, W. R., Cox, C. D., Ballun, M. C., … Strauss, A. M. (2014). Friction stir welding : Process , automation , and control. *Journal of Manufacturing Processes*, *16*(1), 56–73. http://doi.org/10.1016/j.jmapro.2013.04.002

Jordon, J. B., Horstemeyer, M. F., Daniewicz, S. R., Badarinarayan, H., & Grantham, J. (2010). Fatigue Characterization and Modeling of Friction Stir Spot Welds in Magnesium AZ31 Alloy. *Journal of Engineering Materials and Technology*, *132*(4), 41008. Retrieved from http://dx.doi.org/10.1115/1.4002330

Mishra, R. S., & Ma, Z. Y. (2005). Friction stir welding and processing. *Mater. Sci. Eng.*, *50*, 1–78. http://doi.org/10.1016/j.mser.2005.07.001

Schmidt, H. N. B., Dickerson, T. L., & Hattel, J. H. (2006). Material flow in butt friction stir welds in AA2024-T3. *Acta Materialia*, *54*(4), 1199–1209. http://doi.org/http://dx.doi.org/10.1016/j.actamat.2005.10.052

Seidel, T. U., & Reynolds, A. P. (2001). Visualization of the material flow in AA2195 friction-stir welds using a marker insert technique. *Metallurgical and Materials Transactions A*, *32*(11), 2879–2884. http://doi.org/10.1007/s11661-001-1038-1

Yadava, M. K., Mishra, R. S., Chen, Y. L., Carlson, B., & Grant, G. J. (2010). Study of friction stir joining of thin aluminium sheets in lap joint configuration. *Sci. Technol. Weld. Join.*, *15*(1), 70–76. http://doi.org/10.1179/136217109X12537145658733

Yan, J., Xu, Z., Li, Z., Li, L., & Yang, S. (2005). Microstructure characteristics and performance of dissimilar welds between magnesium alloy and aluminum formed by friction stirring. *Scr. Mater.*, *53*, 585–589. http://doi.org/10.1016/j.scriptamat.2005.04.022

Yang, Q., Li, X., Chen, K., & Shi, Y. J. (2011). Effect of tool geometry and process condition on static strength of a magnesium friction stir lap linear weld. *Mater. Sci. Eng. A*, *528*, 2463–2478. http://doi.org/10.1016/j.msea.2010.12.030

Yuan, W., Carlson, B., Verma, R., & Szymanski, R. (2012). Study of top sheet thinning during friction stir lap welding of AZ31 magnesium alloy. *Sci. Technol. Weld. Join.*, *17*(5), 375–381. http://doi.org/10.1179/1362171812Y.0000000018

7. RESPONSIBILITY NOTICE

The authors are responsible for the printed material included in this paper.